AGU ADVANCING EARTH AND SPACE SCIENCES

Water Resources Research

RESEARCH ARTICLE
10.1029/2023WR036076

An Isotope Mass Balance Analysis of Evaporative Loss From Lake Turkana, Kenya Using $\delta^{18}O$ and δD of Natural Waters

M. Saslaw[1], D. Yang[2,3], D. Lee[4], C. J. Poulsen[5], and G. A. Henkes[1,2]

[1]Department of Geosciences, Stony Brook University, Stony Brook, NY, USA, [2]Interdepartmental Doctoral Program in Anthropological Sciences, Stony Brook University, Stony Brook, NY, USA, [3]Department of Geology & Geophysics, University of Utah, Salt Lake City, UT, USA, [4]Department of Earth & Environmental Sciences, University of Michigan, Ann Arbor, MI, USA, [5]Department of Earth Sciences, University of Oregon, Eugene, OR, USA

Key Points:

- New measurements of meteoric waters from the Turkana Basin in northern Kenya plot along the meteoric water line
- A lake water evaporation line is developed using Bayesian modeling applied to a terminal lake mass balance model
- The model enables predictions of lake water δ values under past and future climate change scenarios

Supporting Information:

Supporting Information may be found in the online version of this article.

Correspondence to:

M. Saslaw,
mae.saslaw@gmail.com

Citation:

Saslaw, M., Yang, D., Lee, D., Poulsen, C. J., & Henkes, G. A. (2024). An isotope mass balance analysis of evaporative loss from Lake Turkana, Kenya using $\delta^{18}O$ and δD of natural waters. *Water Resources Research*, *60*, e2023WR036076. https://doi.org/10.1029/2023WR036076

Received 15 AUG 2023
Accepted 21 MAR 2024

Author Contributions:

Conceptualization: M. Saslaw, D. Yang, G. A. Henkes
Data curation: M. Saslaw, D. Yang, D. Lee
Formal analysis: M. Saslaw, D. Yang, D. Lee, G. A. Henkes
Funding acquisition: G. A. Henkes
Investigation: M. Saslaw, D. Yang, D. Lee, G. A. Henkes
Methodology: M. Saslaw, D. Yang, D. Lee, G. A. Henkes
Project administration: D. Yang, G. A. Henkes
Resources: D. Yang, C. J. Poulsen, G. A. Henkes
Software: M. Saslaw

Abstract

Measurements of oxygen and hydrogen stable isotope ratios ($\delta^{18}O$ and δD) in meteoric waters provide insight to overlapping effects of evaporation, precipitation, and mixing on basin scale hydrology. This study of waters collected between 2016 and 2021 in the Turkana Basin, northern Kenya, uses $\delta^{18}O$ and δD to understand water balance in Lake Turkana, a large, low-latitude, alkaline desert lake. The Omo River, a major river system in the Ethiopian Highlands, is historically understood to provide approximately 90% of the water input to Lake Turkana. Discharge of the Omo is prohibitively difficult to measure, but stable isotope ratios in the lake may provide a meaningful method for monitoring the lake's response to changes in input. Precipitation in the Turkana Basin is low (<200 mm/year) with negligible rainfall on the lake's surface, and all water loss from the lake is evaporative. We compare new measurements with previous data from the region and records of lake height and precipitation from the same time period. We show that a Bayesian approach to modeling evaporation using atmospheric conditions and river $\delta^{18}O$ and δD yields results consistent with published water balance models. Continued sampling of lake and meteoric waters in the Turkana Basin will be a useful way to monitor the lake's response to regional and global climate change.

Plain Language Summary

Lake Turkana is the largest desert lake in the world, in one of the hottest and driest places on Earth. Studying and preserving the lake are important because people and ecosystems depend on it, but information is lacking because it is remote and irregularly monitored. Most of the water in Lake Turkana comes from the Omo River, which flows through the Ethiopian Highlands. Lake Turkana has no outlet; therefore, evaporation is the only process that removes water from the lake. In this study, we analyzed samples of lake water as well as rain, river, surface, and ground waters and developed a model that uses measurements of oxygen and hydrogen stable isotopes in the water to help us understand how much evaporation occurs in Lake Turkana. Future lake water monitoring efforts should consider stable isotope methods to record how the basin hydrology responds to climate change.

1. Introduction

Lake Turkana is the largest desert lake in the world. It is the fourth largest of the African Great Lakes, located in the eastern branch of the East African Rift System. Most of the lake lies in Kenya, and the dynamic Omo River delta at the north end of the lake spans both sides of the border between Kenya and Ethiopia (Figure 1). It is a terminal lake with a surface area of 7,560 km^2 and a drainage area of 130,860 km^2, with most of its catchment in the Omo Basin and canonically >90% of its input from the Omo River (Avery, 2012; Hopson, 1982; Nicholson, 2022; Obiero et al., 2022). The southern section of the lake is deepest, around 110 m, and the mean depth is 30 m with shallow shorelines that provide ideal habitats for fish reproduction (Carr, 2017; Hopson, 1982; Olaka et al., 2010). Mean annual air temperatures in the Turkana Basin are among the hottest on the planet, around 30°C, and lake surface temperatures are ∼2°C lower (Morrissey et al., 2017; Passey et al., 2010; Yost et al., 2021). While seasonal air temperatures do not vary greatly, rainfall is seasonal in the Turkana Basin and in the Ethiopian Highlands (Johnson & Malala, 2009; Nicholson, 1996). Mean annual precipitation (MAP) in the basin is 200–300 mm/year and falls mostly in the boreal spring and autumn, typical of the "short" and "long" rains prevalent in eastern Africa (Levin et al., 2009; Nicholson, 1996; Olaka et al., 2010). Strong diurnal winds contribute to circulation of water and vertical mixing in the water column, with temperature gradients that vary seasonally 1–3°C (Hopson, 1982; Johnson & Malala, 2009; Kolding, 1992; Yuretich & Cerling, 1983). Because the lake is long but shallow, lake surface temperature is consistent, with a gradient from north to south <4°C (Morrissey et al., 2017),

Supervision: G. A. Henkes
Validation: M. Saslaw, D. Yang, D. Lee, G. A. Henkes
Visualization: M. Saslaw
Writing – original draft: M. Saslaw
Writing – review & editing: M. Saslaw, D. Yang, D. Lee, C. J. Poulsen, G. A. Henkes

and the blue-green algae that give the water its famous jade color are transported from the nutrient-rich Omo River delta throughout the lake (Johnson & Malala, 2009).

In such hot, arid, and remote conditions, Lake Turkana provides resources for communities on the lakeshore and surrounding areas. The water is too saline for people to drink, but livestock and fish depend on it. The estimated population of the Turkana region is approximately 1 million people, whose livelihoods are based on pastoralism, fishing, and, to a lesser extent, crop farming (Avery, 2014). Water resource management is complex, and a source of both local and international conflict, as Ethiopia manages the Omo River and its catchment while Kenyans in the Turkana Basin and Ethiopians in the Lower Omo Valley face downstream effects of dams and diversions along the river. The Gilgel Gibe Dam project is part of Ethiopia's Climate Resilient Green Economy plan, intended to provide electricity to tens of millions of people in Ethiopia, Kenya, Sudan, and Djibouti (Schapper, 2021). Human Rights Watch, an international non-governmental organization, estimates that hundreds of thousands of indigenous people in the Lower Omo region have been displaced by development of sugar plantations and flooding of their ancestral lands as the project reshapes the landscape (Horne, 2012). In addition to modulating the volume of water flowing into the lake, damming changes the timing of flood pulses that deliver water and sediment—an estimated 60%–65% of the water from the Omo River that enters Lake Turkana is delivered during the river's flood stage (Yuretich & Cerling, 1983). Fish need these regular cycles of disturbance, and there is a risk of fisheries habitat loss without dam and irrigation project management that considers downstream ecological impacts (Gownaris et al., 2017). Monitoring water flux in the lake is therefore critical to understanding how hydrologic changes in Lake Turkana's main tributary affect people's lives.

Three national parks surrounding Lake Turkana—Sibiloi National Park, Central Island National Park, and South Island National Park—are designated as UNESCO World Heritage in Danger sites under threat of damage from the Gilgel Gibe Dam project as well as other planned agricultural and transportation projects (UNESCO, 2018). Hominin fossil sites surrounding the lake also draw international attention for the region and motivate paleoclimate research in Turkana (Wood & Leakey, 2011). Archeological sites on paleoshorelines near modern Lake Turkana contain records of the development of some of the earliest societies and cultures, including early burials, monument building (Hildebrand et al., 2018), and warfare (Lahr et al., 2016). The basin has been a place of change, adaptation, and development for people living around it for millions of years.

The water level of Lake Turkana has fluctuated 50–100 m during the Holocene, as the latest in a series of lakes that have filled the basin (Bloszies et al., 2015; Feibel, 2011; Forman et al., 2014). The most recent high stand at 80 m above the current lake level occurred toward the end of the African Humid Period, about 6 ka (Garcin et al., 2012; van der Lubbe et al., 2017). In the past 1,000 years, high stands have been limited to 20 m above modern (Bloszies et al., 2015). Orbital forcing influences hydroclimate, with periods of low and high eccentricity corresponding to changes in seasonal insolation (Lupien et al., 2020). Today, subtle changes in lake depth and shoreline morphology affect the lake's ecosystems, specifically the fish populations that require shallow water habitats (Gownaris et al., 2018). A decrease in lake level by 25 m or more would be catastrophic for fish, and a decrease greater than 40 m would bifurcate the present-day lake and expose the lake bottom across the narrow southern section (Carr, 2017).

Lake Turkana is unique among African lakes in that it is alkaline (pH = 9.3), saline (total dissolved solids = 2500 ppm), shallow, and receives only negligible amounts of water from precipitation over the lake, so studies of other basin-scale water balance in other rift basin lakes are often not applicable (Nicholson, 2022; Yuretich & Cerling, 1983). Due to the difficulty in accessing the lake (i.e., one small commercial airport serves the entire basin from Lodwar, Kenya), much of the current understanding of lake level dynamics is based on remotely sensed data from the United States Department of Agriculture (USDA) and from surveys and geochemical studies performed in the last 50 years. Satellite imagery is integrated from multi-year records and different instruments, and the elevations recorded in remote data sets for Turkana are not referenced to geodetic points, and thus problematic for mass balance analysis.

Stable isotope hydrology provides established methods for studying the water cycle at regional and global scales. Rare, heavy isotopes of oxygen and hydrogen (^{18}O and ^{2}H, or D for deuterium) in water fractionate according to predictable physical processes; during evaporation, molecules containing only lighter isotopes (^{16}O and H) will change phase preferentially, resulting in liquid water that is "enriched" in ^{18}O and D relative to its source (Criss, 1999; Dansgaard, 1964; Gat, 1995, 1996; Rozanski et al., 1992). Delta notation is an expression of the

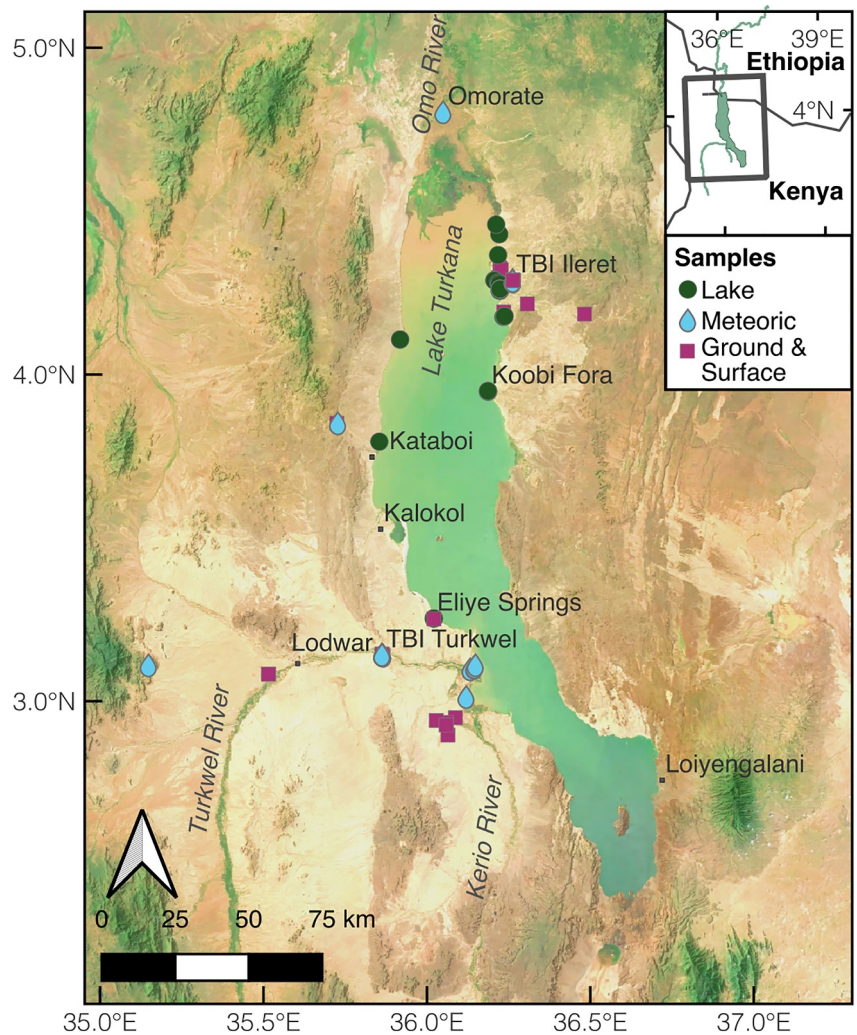

Figure 1. Sample location map for waters collected in the Turkana Basin from 2016 to 2021. The waters are shown as three different symbols, simplifying the types of water collected for analysis. Lake water samples (green circles) were collected from the lake shoreline. Lake Turkana appears as an aquamarine area in the center of the map with no topography. The north end of the lake is characterized in this image by a transition from the blush-colored deltaic sediment plume to the rest of the lake. Satellite imagery from MapTiler was enhanced for higher contrast. The map inset in the upper right places Turkana within the national borders of Kenya and Ethiopia.

isotope ratios ($^{18}O/^{16}O$ and D/H in this case) compared to the same ratios in a reference material (Vienna Standard Mean Ocean Water [VSMOW] for low latitude waters), given as ‰ (per mil):

$$\delta = \left(\frac{R_{\text{sample}}}{R_{\text{standard}}} - 1\right) \times 1000 \quad (1)$$

Ratios of $^{18}O/^{16}O$ and D/H in waters from lake catchments are sensitive to differences in water sources and the extent of evaporation, so measuring $\delta^{18}O$ and δD in lake samples over time is a useful way to track the effects of evaporation and change in mass balance. Knowing the isotope ratios of input waters thus enables an estimate of evaporative losses because the relative enrichment of lake waters in ^{18}O and D is a function of what proportion of water has evaporated; light isotopologues evaporate preferentially, increasing $\delta^{18}O$ and D in the remaining reservoir (Gat, 1995; Gibson et al., 2008). Deuterium excess (d-excess) is a measure of deviation from the reference slope relating $\delta^{18}O$ and δD in global meteoric waters (Clark & Fritz, 1997; Dansgaard, 1964), defined as:

$$\text{Deuterium excess} = \delta\text{D} - 8\delta^{18}\text{O} \quad (2)$$

Lake water isotope mass balance models use this relationship to evaluate the offset between evaporating lake waters and meteoric source waters (Brooks et al., 2012; Gat, 1995; Gibson et al., 2016). The Global Meteoric Water Line (GMWL) represents the linear relationship, with a slope of 8 (Equation 2) between δ^{18}O and δD under the full range of Earth surface conditions. Notably, elevated δ values in the Ethiopian Highlands were observed when the GMWL was first established and applied (Craig, 1961). Recent isotope hydrology studies across the region quantify trends and interpret stable isotope data from precipitation in Ethiopia (Bedaso et al., 2020; Levin et al., 2009), aquifers and the Turkwel River system (Tanui et al., 2023), and the lake at Ferguson's Gulf, a shallow body of water on the western shore (Beck et al., 2020), but water isotope data from Lake Turkana specifically remain sparse. This study uses δ^{18}O and δD of natural waters from the Turkana Basin, including precipitation, river waters, and the lake, to characterize water isotope variability in the remote, semi-arid region in and around Lake Turkana, and thereby provide a basis for lake water stable isotopes as an indicator of overall basin hydrological balance.

In addition to its importance in modern Kenya, the Turkana Basin hosts a sedimentary record that extends back to at least the Oligocene epoch (Morley et al., 1999) with authigenic carbonate minerals formed in the critical zone (Gathogo & Brown, 2006; Rasbury et al., 2021), lacustrine sediments (Cerling et al., 1988; Feibel, 2011; Garcin et al., 2012), pedogenic carbonates (Cerling, Wynn, et al., 2011; Levin et al., 2011; Passey et al., 2010; Wynn, 2000), and fossil teeth (Cerling et al., 2003; Cerling, Levin, et al., 2011; Green et al., 2022; Harris et al., 2008; Levin et al., 2006). A detailed understanding of stable isotopes in the modern lake also provides context for the interpretations of paleoenvironments derived from stable isotopes of sedimentary rocks (Cerling et al., 1988; Passey et al., 2010).

2. Materials and Methods

2.1. Sample Collection and Stable Isotope Measurements

Waters analyzed in this study were collected between September 2016 and July 2021 by the authors and collaborators working at the Turkana Basin Institute (TBI) Turkwel and Ileret field stations (Figure 1). Kale ("kah-LAY") Beach, our most frequently visited Lake Turkana water sampling site, is a section of eastern lake shoreline approximately 35 km south of the Omo River delta. All lake samples from Kale Beach and other sites were taken near shore, in areas where lake depth ranged from 1 to 2 m and within or just lakeward of the shore wave zone. River water samples from the Turkwel River were collected close to the river's center line, where flow was moderate, and water was at least 0.5 m deep. The Omo River was sampled from the shore near the town of Omerate under low-flow, sediment-rich water conditions. Precipitation was collected opportunistically, as rainfall sufficient to yield a ∼2 mL sample was infrequent (Leakey et al., 2023). Available containers for rainwater, mainly plastic, conical, graduated rain gauges, were monitored and emptied into vials immediately after rainfall ceased in order to minimize surface evaporation from the collectors. Two of the precipitation samples were stored overnight in vials that were loosely sealed (MSTI006, MSTI008; Table S1); when analyzed, these samples were shown to have abnormally low δD values, and thus have been excluded from the discussion due to inconsistent preparation and evident isotope fractionation following collection. Some precipitation samples were collected from roof gutters at TBI-Ileret and TBI-Turkwel, or from an access point where rainwater flows from the roof into the building cisterns. This style of collection implies that building roofs were saturated with rainwater, which is only possible during a heavy rain event.

With exception of the aforementioned precipitation samples, water samples were collected using 5 ml plastic syringes and filtered through 0.45 μm PTFE filters into 2 mL glass vials with phenolic cone displacement caps for transport and storage. Vials were sealed in individual Whirl-pak bags to prevent evaporation or water loss during transport, then sealed with parafilm upon return to the laboratory. Some samples, noted in Table S1, were not filtered in the field but contained no visible algal growth or sediment (suspended or settled). These were filtered in the laboratory before isotopic analysis.

Stable isotope ratios of oxygen and hydrogen in the filtered waters were measured in three facilities. Samples collected in 2016 were measured by high temperature conversion elemental analyzer isotope ration mass spectrometry (TC/EA-IRMS) at the Boston University Stable Isotope Laboratory in early 2017, calibrated and

corrected using IAEA OH-14, 15, 16. Samples collected from 2017 to 2020 were measured on a Picarro 2130i cavity ring down laser spectroscopy (CRDS) analyzer coupled to a vaporization module and Picarro autosampler at the University at Buffalo Organic and Stable Isotope Laboratory, run with three in-house standards. Data was corrected using Picarro post run corrections and in-house standards according to van Geldern and Barth (2012). Samples collected in 2021 were measured at the University of Michigan Climate Change Research Group on a similar Picarro 2130i CRDS and corrected using Picarro ChemCorrect for VSMOW-SLAP scale calibration with USGS reference waters USGS 45, 46, 49, and 50 and four in-house liquid standards (Aron et al., 2021). Precision for measurements in all laboratories was better than 0.1‰ for $\delta^{18}O$ and 0.3‰ for δD.

2.2. Lake Evaporation Model

As a terminal lake, all water loss from Lake Turkana is evaporative. Using a 4000-year record of oxygen isotope measurements combined with modern observed evaporation rates and environmental conditions, Ricketts and Johnson (1996) established an isotope mass balance model for Lake Turkana. Their model showed that lake water isotopes have fluctuated as a result of 10–20 m lake level changes, water source, and changes in the rates of inflow and outflow. Because the lake does not appear to be sensitive to small fluctuations on the order of 2 m, we assume the lake is at hydrogen and oxygen isotope steady state in our related modeling effort. Our new lake water measurements do not capture variability with latitude or depth, but we are able to model boundary layer conditions using a set of informative prior assumptions described in detail in Supporting Information S1. We build on previous isotope mass balance studies by using a Bayesian approach along with present day lake conditions.

A local evaporation line (LEL) predicts isotope ratios in an evaporating body of water as a function of isotopic and environmental inputs. We apply a simple mass balance model for large lakes (Gibson et al., 2016), adapted for the basic environmental conditions of Lake Turkana. Our Bayesian approach produces an LEL from predicted lake water isotope ratios for $\delta^{18}O$ and δD as follows:

$$\delta_L = \frac{\delta_i + mx\delta^*}{1 + mx}(‰) \tag{3}$$

where x is the ratio of evaporation over inflow ($x = 1$ in terminal lakes), δ_i is the isotope ratio of input (river) waters, m is the enrichment slope at a specified temperature and humidity:

$$m = \frac{rh - 10^{-3} \cdot (\varepsilon_K + \varepsilon^+/\alpha^+)}{1 - rh + 10^{-3} \cdot \varepsilon_K} \tag{4}$$

and δ^* is the limit of isotopic enrichment, the end-member composition as a body of water desiccates:

$$\delta^* = \frac{rh \cdot \delta_A + \varepsilon_K + \varepsilon^+/\alpha^+}{rh - 10^{-3} \cdot (\varepsilon_K + \varepsilon^+/\alpha^+)}(‰) \tag{5}$$

rh is relative humidity expressed as a fraction between 0 and 1, ε_K is the diffusion controlled fractionation at rh as defined by Horita et al. (2008), and ε^+/α^+ is the equilibrium isotopic separation over liquid-vapor fractionation factor at a given air temperature (Horita & Wesolowski, 1994):

$$\varepsilon^+ = \left(\alpha^+ - 1\right) \cdot 1000 \tag{6}$$

Temperature and relative humidity are primary controls for evaporation in any system, and in addition to the input isotopic composition, the mixing of water vapors from the lake and atmosphere influences isotopic evolution from source water to fully evaporated. δ_A represents the boundary layer vapor into which the lake evaporates, estimated as:

$$\delta_A = \frac{\delta_P - k\varepsilon^+}{1 + 10^{-3} \cdot k\varepsilon^+}(‰) \tag{7}$$

where k is the fraction (from 0 to 1) of isotopic equilibrium between the lake water and atmosphere such that seasonal lakes are close to 0.5, and non-seasonal lakes close to 1; and the boundary layer vapor (δ_A) is assumed to be in isotopic equilibrium with mean annual precipitation (δ_P). For large lakes such as Lake Turkana, the value of δ_A also evolves as lake water evaporates. Increasing moisture buildup affects rh, m, δ^*, and lake evaporation (δ_E), and thus the enrichment slope (Gibson et al., 2016; Jasechko, 2019). To account for this, we iterate solutions to the following equations over a fraction of lake water evaporate (f) in the atmosphere:

$$\delta'_A = (1-f)\cdot\delta_A + f\cdot\delta'_E(‰) \tag{8}$$

where the value of δ'_E also evolves with changing rh and δ'_A as follows:

$$\delta'_E = \frac{(\delta_L - \varepsilon^+)/(\alpha^+ - (rh\cdot\delta'_A) - \varepsilon_k)}{1 - rh + (10^{-3}\cdot\varepsilon_k)}(‰) \tag{9}$$

Additional equations for mixed vapor values and increasing rh with f are provided in Supporting Information S1. We estimate priors for environmental conditions and input isotope ratios from all available data (see Text S1 in Supporting Information S1) and implement the series of equations above using the Bayesian inference Using Gibbs Sampling (BUGS) language (Lunn et al., 2012). Details for the Markov-Chain Monte Carlo (MCMC) simulation, including chain convergences and bivariate densities, are also provided in Supporting Information S1.

We tested the sensitivity of the model to bias in our sample locations (i.e., our data is concentrated in the northern portion of lake) by adding 1‰ to our measured $\delta^{18}O$ and adjusting δD along the LEL accordingly. This corresponds to the trend observed in a latitudinal study of lake water ostracods isotopes (Ricketts & Johnson, 1996; Thirumalai et al., 2023). The estimate for f, the fractional contribution of lake water evaporation to rh (Equation 8), is sensitive to this change: as expected, f increases when lake water isotopes shift toward higher values. Additional sensitivity tests and results are described in Supporting Information S1; these reveal that the model is sensitive to the prior δ values of inflow, precipitation, and lake water, and not sensitive to the prior distributions of temperature, rh, or evaporative seasonality, k (Table S2 in Supporting Information S1). All code authored for this study is available on GitHub (Yang et al., 2024).

3. Data

Samples collected by the authors and collaborators 2016–2021 (n = 133) include meteoric and groundwaters (Table S1). Summary statistics for meteoric waters are shown below in Table 1. Figure 2 shows distributions of different water types compared to the GMWL.

Stable isotope measurements from Lake Turkana are shown chronologically in Figure 3 with lake height data from Global Reservoirs and Lakes Monitor (G-REALM) satellite altimetry and local precipitation measured by TBI researchers and residents at both the Ileret and Turkwel field stations (Leakey et al., 2023). There is a notable gap in sample collection between January 2020 and June 2021 due to work restrictions in response to the global COVID-19 pandemic. During this same period, for reasons that are not yet well understood, the height of Lake Turkana increased by approximately 2 m, causing major disruptions to lake shoreline communities. This increase in the lake level corresponds to a change in volume of approximately 20 km^3 (9.8% of lake volume) according to the lake height/volume relationship defined by Avery (2010). Such a trend was unexpected given both the drought conditions and increasing water consumption for agriculture in Ethiopia along the Omo River; future sampling as the lake level remains high (Figure 3a) and eventually recedes will be useful for understanding correlation between lake level and water isotopes.

4. Results

4.1. Precipitation and River Water Isotopes

The sources of water vapor and precipitation differ between the catchment of the Omo River in the Ethiopian Highlands and the scant rainfall over and around Lake Turkana. Precipitation in Ethiopia is notably enriched in ^{18}O with low d-excess values, consistent with a recycled water source from the Congo Basin (Levin et al., 2009), whereas water vapor in Turkana originates in the Indian Ocean and is transported inland by the Turkana Jet, a low-

Table 1
Representative Values and Statistics for Meteoric Waters Collected From the Turkana Basin

Water source	*n*	Mean $\delta^{18}O$	$\delta^{18}O$ SD	Min. $\delta^{18}O$	Max. $\delta^{18}O$	Mean δD	δD SD	Min. δD	Max. δD	Mean d-excess
Lake	49	5.2	0.6	2.6	6.6	36.8	3.3	23.1	42.6	−4.6
Kale Beach	33	5.1	0.6	2.6	6.6	35.8	3.3	23.1	40.7	−4.7
Koobi Fora	5	5.5	0.3	5.2	5.9	38.8	0.9	37.3	39.7	−5.1
Eliye Springs	3	5.2	0.2	5.0	5.5	38.9	2.1	36.5	40.3	−2.6
Nariokotome	2	5.2	0.6	4.8	5.6	38.0	3.0	35.9	40.1	−3.6
Sericho	2	6.1	0.3	5.9	6.4	42.2	0.5	41.9	42.6	−6.9
Il Eeriet Delta	1	5.5				39.8				−4.0
Il Kimere Delta	1	5.6				40.0				−5.0
Topernawi	1	4.7				32.2				−5.5
Tulu Bor Delta	1	5.2				37.3				−4.5
Delta	6	−0.3	1.1	−0.6	2.2	5.2	4.3	3.2	14.0	6.3
Kerio River Delta	1	2.2		2.2	2.2	14.0		14.0	14.0	−3.7
Turkwel River Delta	5	−0.6	0.0	−0.6	−0.6	3.5	0.2	3.2	3.6	8.2
River	13	−0.9	1.3	−3.4	1.4	0.1	10.3	−26.2	10.3	7.5
Turkwel River	10	−0.7	1.1	−2.2	1.4	1.8	6.4	−8.0	10.3	7.7
Omorate	1	−0.4				8.9				11.8
Topernawi	1	−3.4				−26.2				0.9
Precipitation	28	0.9	2.3	−3.0	5.9	9.9	15.1	−26.3	36.4	3.1
TBI-Ileret	26	0.8	2.3	−3.0	5.9	9.2	15.3	−26.3	36.4	3.1
TBI-Turkwel	2	2.2	1.7	0.9	3.4	19.7	5.3	16.0	23.5	2.5

Note. All δ values are reported in the ‰ notation relative to VSMOW.

level jet stream. The jet creates strong winds across approximately 700 km of low elevation desert terrain from the Indian Ocean to South Sudan, northwest of Lake Turkana, known as the Turkana Channel (Munday et al., 2022; Nicholson, 2016). When the jet is at its strongest during the boreal summer, rainfall is limited. The long and short rains occur in the transition seasons when the jet is weaker and more vapor rains out in the Turkana Channel (Munday et al., 2022; Vizy & Cook, 2019). In Ethiopia and Kenya, these seasonal patterns depend on the stability of broader regional, continental, and marine climatological cycles. Precipitation records from years prior to the range of this study (Leakey et al., 2023) and local observations (Derbyshire et al., 2021; Junqueira et al., 2021) indicate the regional climate is trending toward decreased annual rainfall, less pronounced seasonal rains, and longer droughts.

Mean isotope ratios for precipitation are $\delta^{18}O = 0.9‰$ and $\delta D = 9.9‰$, comparable to those published by Levin et al. (2009) for northern Kenya (mean $\delta^{18}O = -0.6‰$ and $\delta D = 10.1$ ‰). While isotope ratios of precipitation have a broad range (8.9‰ for $\delta^{18}O$ and 62.6‰ for δD), most fall below the GMWL, which may indicate sub-cloud evaporation under arid conditions with high winds (e.g., we have occasionally observed virga, an end-member case of precipitation evaporation, while conducting field campaigns in Turkana). For those precipitation samples that have rainfall amounts recorded on the day of collection ($n = 16$; these are not directly associated measurements), the highest $\delta^{18}O$ and δD values are associated with precipitation rates below 25 mm/day (Figure 4). Eight samples represent rain events <10 mm, and all but three are <30 mm.

Omo River isotope values published by Levin et al. (2009) include two samples from September 1979, one from 1999, and two from 2004, one of which does not include a δD value. All samples were taken from the river near Shungura, approximately 30 km north of the lake. The ranges of reported values for Omo River $\delta^{18}O$ and δD are −2.9–0.5‰ and 4.0–17.3‰, respectively, but because the collection dates in 1979, 1999 and 2004 are unknown we do not know to what degree that range reflects a combination of inter- or intra-annual variability. This study includes one sample (V02) obtained from the river approximately 20 km north of the lake at Omorate in 2016. Our Omo River sample ($\delta^{18}O = -0.4‰$, $\delta D = 8.9$) was collected between the long and short rains, during the boreal

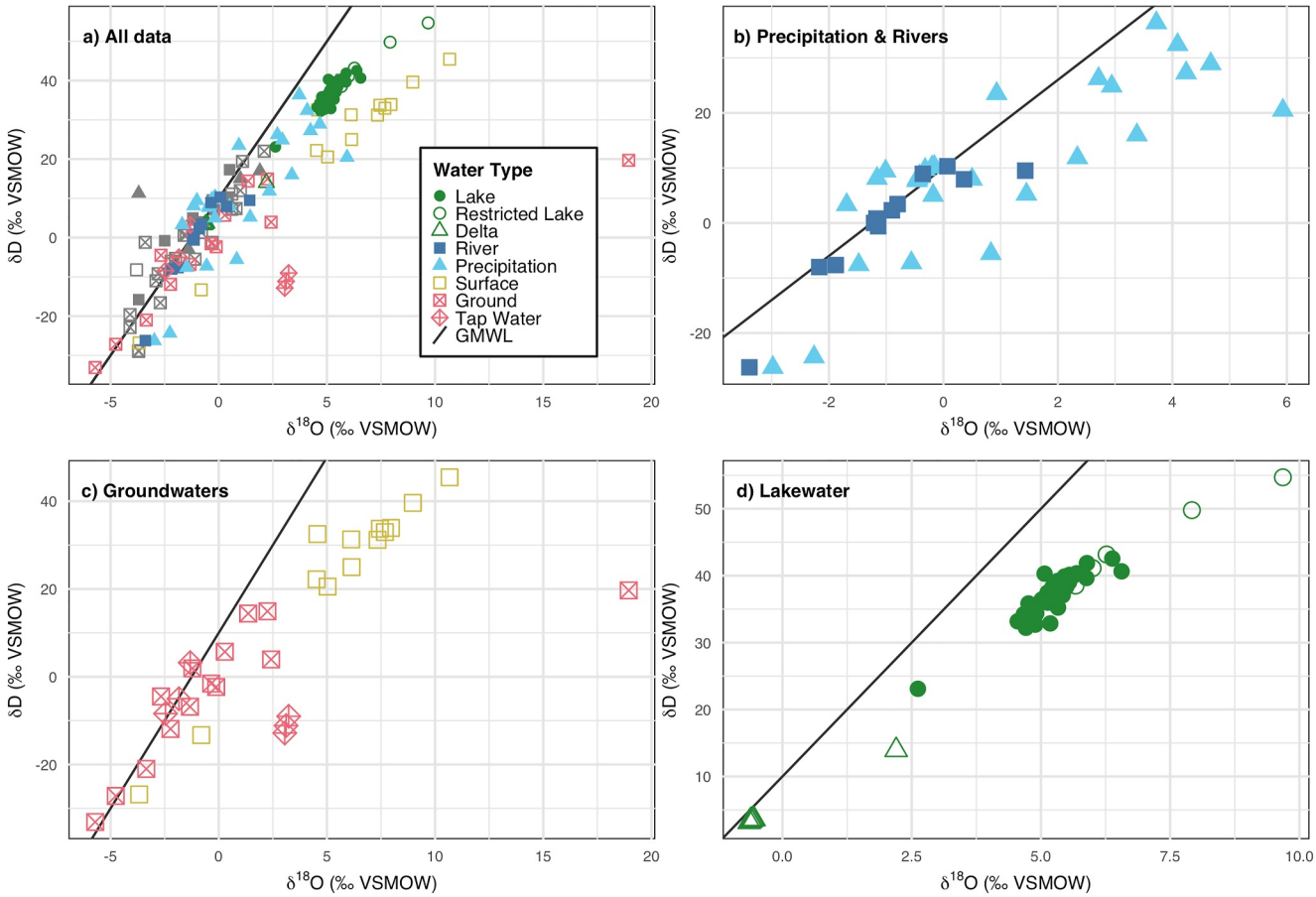

Figure 2. Water isotope measurements from this study shown with Global Meteoric Water Line and sample data from Levin et al. (2009) from northern Kenya and the Omo River (gray data points). Note that the *x*- and *y*-axes differ for each sub-plot.

midsummer, thus it is likely our single measurement neither reflects the lowest seasonal δ values expected during the rainy seasons nor the highest seasonal values expected during the boreal winter dry season. We were unable to sample the Omo River extensively for this study due to geopolitical conditions at the border and in Ethiopia.

The majority of river water measured in this study was sampled from the Turkwel River at the TBI-Turkwel research center, approximately 30 km east (lakeward) from Lodwar, Kenya. Mean $\delta^{18}O$ and δD for the Turkwel are $-0.7‰$ and $1.8‰$ respectively (Table 1). The temporal resolution of this data is too low to resolve interannual or seasonal trends, which might be expected because of the reduced incidence of heavy rain events after early 2019 in the local precipitation data sets (Figure 3b; Leakey et al., 2023). The Turkwel River is the second-largest input into Lake Turkana, and reliable access at multiple points (e.g., Lodwar, Kenya and the TBI-Turkwel facility) enables an ongoing sampling campaign that will extend beyond the temporal range of this data set. New analysis of stable isotope measurements from the Turkwel River at Lodwar demonstrates the importance of the Turkwel in recharging the shallow alluvial aquifer, especially during the wet season (Tanui et al., 2023). Because the river integrates precipitation isotopes, river water measurements can also be a proxy for precipitation isotope values over time in the Turkwel River watershed, where precipitation collection is challenging.

4.2. Groundwater Isotopes

Groundwaters were collected opportunistically during geologic field work from natural water holes, hand-dug wells, drilled wells, and tap water at the TBI research centers (Figure 1). Average $\delta^{18}O$ and δD for all groundwaters ($n = 20$) are $0.4‰$ and $-4.6‰$, respectively. One groundwater sample had anomalously high values—$19.0‰$ $\delta^{18}O$ and $19.7‰$ δD, respectively. This sample was collected from a saline well, unlike every other sample. Most samples plot along the GMWL, overlapping with rainwater and river samples (Figure 2), yet the

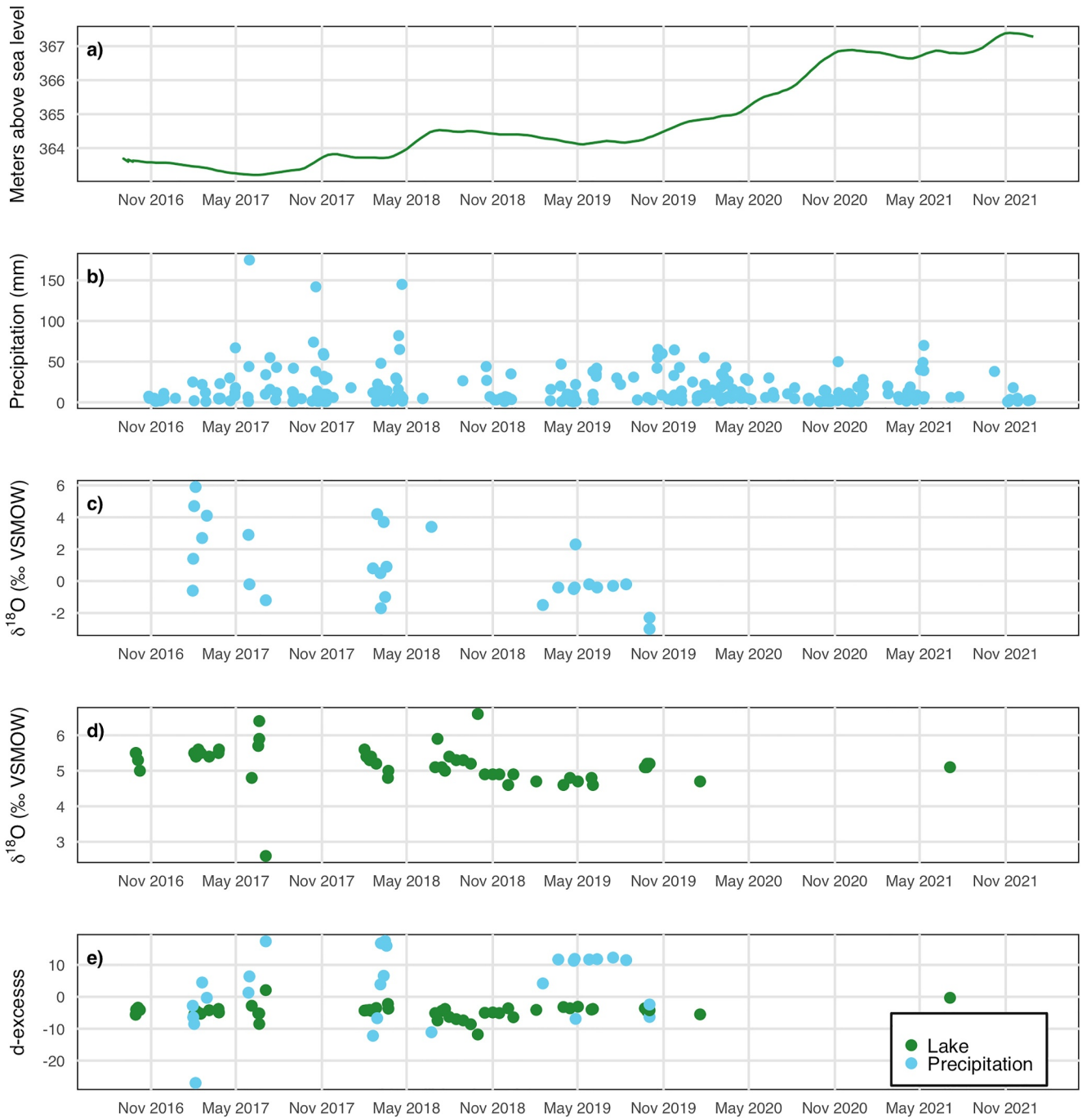

Figure 3. (a) Lake water elevation (in meters above sea level or masl) from G-REALM satellite remote sensing product for Lake Turkana (USDA/NASA G-REALM, 2023). (b) Precipitation recorded at TBI research centers (Leakey et al., 2023). (c) Precipitation $\delta^{18}O$. (d) Lake Turkana $\delta^{18}O$. (e) d-excess from precipitation and lake water measurements. There is a notable data gap in lake water data from 2020 to mid-2021 because of COVID-19 pandemic travel restrictions.

broad range in ground and tap water isotopes — $\delta^{18}O$ ranges −5.7–19.0‰ and δD ranges −33.1–19.7‰ — reflects variety in groundwater sources. Tap water at TBI-Ileret is pumped from a borehole approximately 140 m deep and reaches the surface at elevated temperatures. The average values for Ileret tap water (n = 3) are $\delta^{18}O$ = 3.1‰ and δD = −11.0‰, an offset from the GMWL that indicates water-silicate interactions at high temperatures (Criss, 1999; Jasechko, 2019). This is also consistent with internal water quality assessments of this well that found concentrations of F, Cl, and Na 20–800 times higher than natural spring waters in the western part of the Turkana Basin (e.g., Eliye Springs). The sample from a saline well at Lothagam (MSTI014) is an example

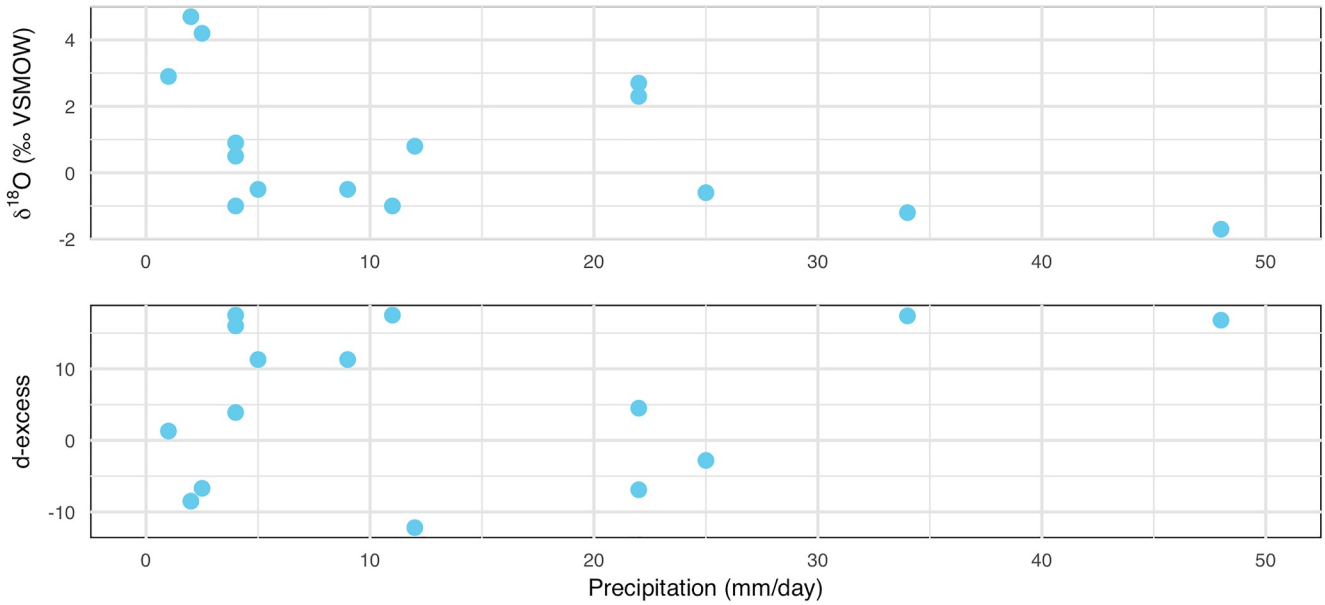

Figure 4. Oxygen isotope ratios and d-excess values for precipitation samples collected on dates with associated total daily rainfall amounts recorded at the TBI-Turkwel or the TBI-Ileret field stations (Leakey et al., 2023). Lower $\delta^{18}O$ values are associated with larger rain events (per day), consistent with an "amount effect" or evaporative effects on precipitation.

of the extent of rock-water oxygen isotope exchange observable in Turkana, with $\delta^{18}O$ offset over 17‰ from the GMWL. In contrast, ground and tap waters from the Turkwel River watershed fall along the GMWL (Figure 2) and closely match meteoric waters because the shallow reservoirs are not likely influenced by geothermal fluids. Three of the surface and ground water values are lower than the lowest measured precipitation or river water values, implying either a source for those fluids that is less evolved than the typical Indian Ocean water vapor that contributes most of the region's meteoric waters (Levin et al., 2009) or an ancient meteoric water source that reflects climate conditions different from present day, for example, during the African Humid Period when the lake shoreline was 70 m higher (van der Lubbe et al., 2017) under a more mesic hydrologic regime covering the rift basin in most of eastern Africa (Tierney et al., 2011). A recent study of groundwaters in the Lodwar Alluvial Aquifer System identifies three distinct isotopic signals—shallow, intermediate, and deep—with no apparent connections to the lake (Tanui et al., 2023). Tap waters from TBI-Turkwel ranged from $\delta^{18}O = -1.3$ to -2.3‰, consistent with their shallow aquifer values ($\delta^{18}O$ range = -2.92–0.25‰), while two samples retrieved from hand-dug wells ($\delta^{18}O = -3.4$ and -5.7‰) may represent the "Scoop Holes" category in their study ($\delta^{18}O$ range = -3.95 to -1.75‰) or have a more negative source that falls outside of their study area (ibid.).

4.3. Lake Turkana Isotopes and Model Results

Of the 49 samples from Lake Turkana, 33 were collected at Kale Beach along the northwest shoreline (Figure 1). Mean values at Kale Beach are $\delta^{18}O = 5.1$‰ and $\delta D = 35.8$‰, and $\delta^{18}O = 5.4$‰ and $\delta D = 38.3$‰ for all other sites combined. All sites are in the northern half of the lake except for Eliye Springs Resort ($n = 3$). The lowest values measured were $\delta^{18}O = 2.6$‰ and $\delta D = 23.1$‰, from a sample collected at Kale Beach the day after a heavy rain (34 mm measured at TBI-Ileret). The highest values were also obtained from Kale Beach and Sericho, another northern site ($\delta^{18}O = 6.6$‰ and $\delta D = 40.7$‰, $\delta^{18}O = 6.4$‰ and $\delta D = 42.6$‰ respectively). We derived an LEL for Lake Turkana using the isotope mass balance model for steady-state, terminal lakes described above (Section 2.2), and our results show that this model produces well constrained estimates of environmental parameters that are consistent with our lake water data. The slope of the LEL (5.39) is steeper than Gibson et al. (2016) predict for low-latitude, arid lakes, and closer to their temperate, large lake slope because of the inclusion of lake water evaporation-derived atmospheric moisture (Equations 8 and 9). Our result is consistent with findings from a review of global lake water isotope measurements that estimated slopes of 5.4 for lakes in arid environments (Vystavna et al., 2021).

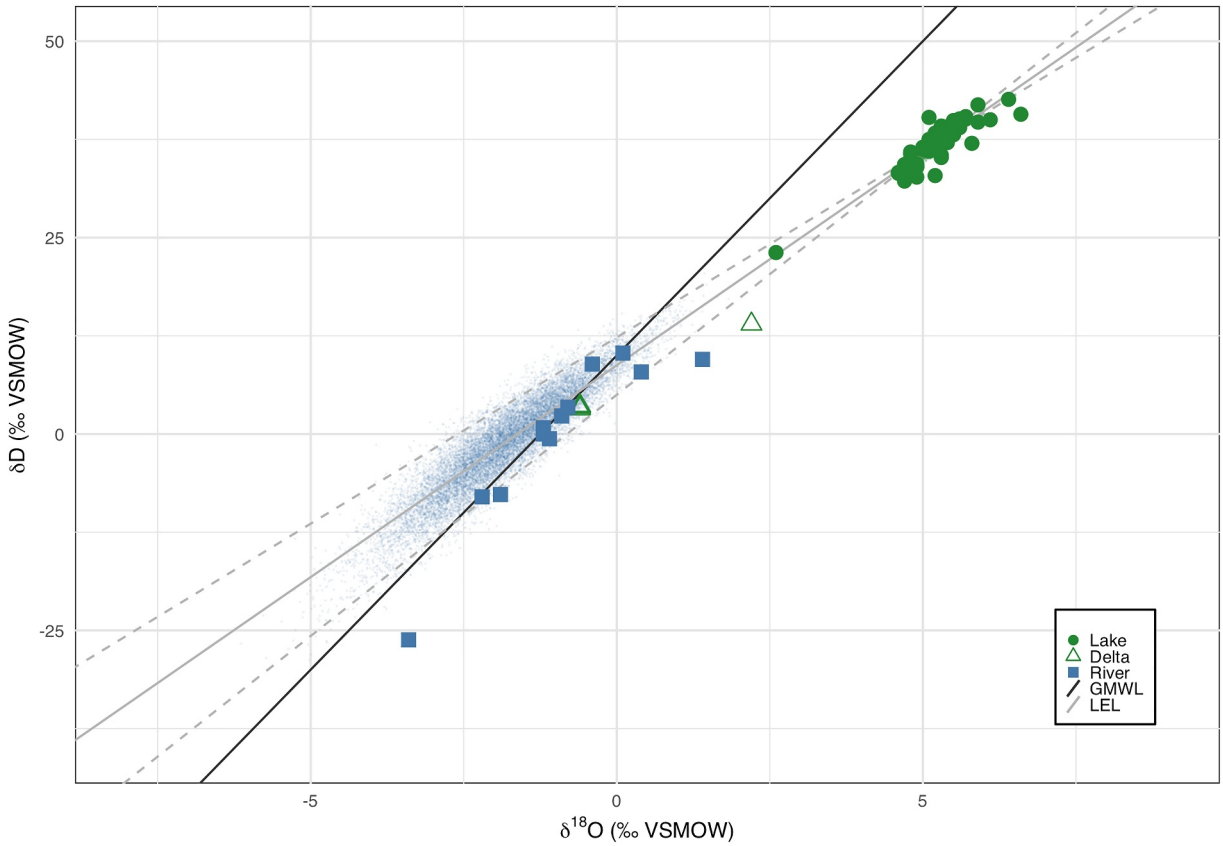

Figure 5. Lake water data with modeled distribution of inflow along the LEL (slope = 5.39). Dashed gray lines are confidence intervals for the model LEL. The cloud of blue data points shows model posteriors for river input δ values; posteriors for evaporated lake water are obscured behind the data points. All posterior distributions, including environmental parameters and isotope values for simulated vapor, are detailed in Supporting Information S1.

5. Discussion and Conclusions

5.1. Implications of Model Results

The Bayesian model explores all possible combinations in the multivariate parameter space, so the posterior distributions of some parameters may differ from their priors when the model is evaluated against the data. These deviations indicate how well constrained the parameters are, as well as any biases in the prior parameter estimations. Figure 6 shows comparisons between prior and posterior distributions in selected parameters; most posterior distributions conform to priors, with small differences observed for relative humidity, $\delta^{18}O_i$, $\delta^{18}O_p$, and δD_p. The difference between our prior estimate of 0.6 for upwind *rh* (Hopson, 1982) and posterior (0.8) most likely indicates higher *rh* for air above the lake surface (Figure 6b), and the further increase in downwind *rh* shows the effect of moisture accumulation in the air over the lake (Figure 6c). The posterior $\delta^{18}O_i$ values are lower than our priors, and centered above the GMWL, whereas the measured river waters are along or below the GMWL (Figure 5). This shift may be explained by the overall lack of constraints on δ_i (see Text S1 in Supporting Information S1 for more discussion of this prior) and could be ameliorated by future stable isotope measurements from the Omo River. We also observe lower $\boldsymbol{\delta}$ values in the posterior estimates for δ_p (Figure 6f), which may indicate that the assumption of equilibrium between atmospheric vapor and amount-weighted MAP may not hold true in the Turkana hydrological system.

In recent decades, annual fluctuations in lake level as observed in satellite imagery amount to about 1–1.5 m of evaporative loss, or 7.6–11.3 km^3/yr (Obiero et al., 2022), ~40% of the volume of annual inflow (19 km^3/yr). By demonstrating the efficacy of the model in predicting *f*, thus constraining the lake evaporation process using isotope mass balance, we provide a new approach for interpreting water isotopes in Lake Turkana. More work is required to validate the model results using direct measurements of *rh* above and adjacent to the lake, lake

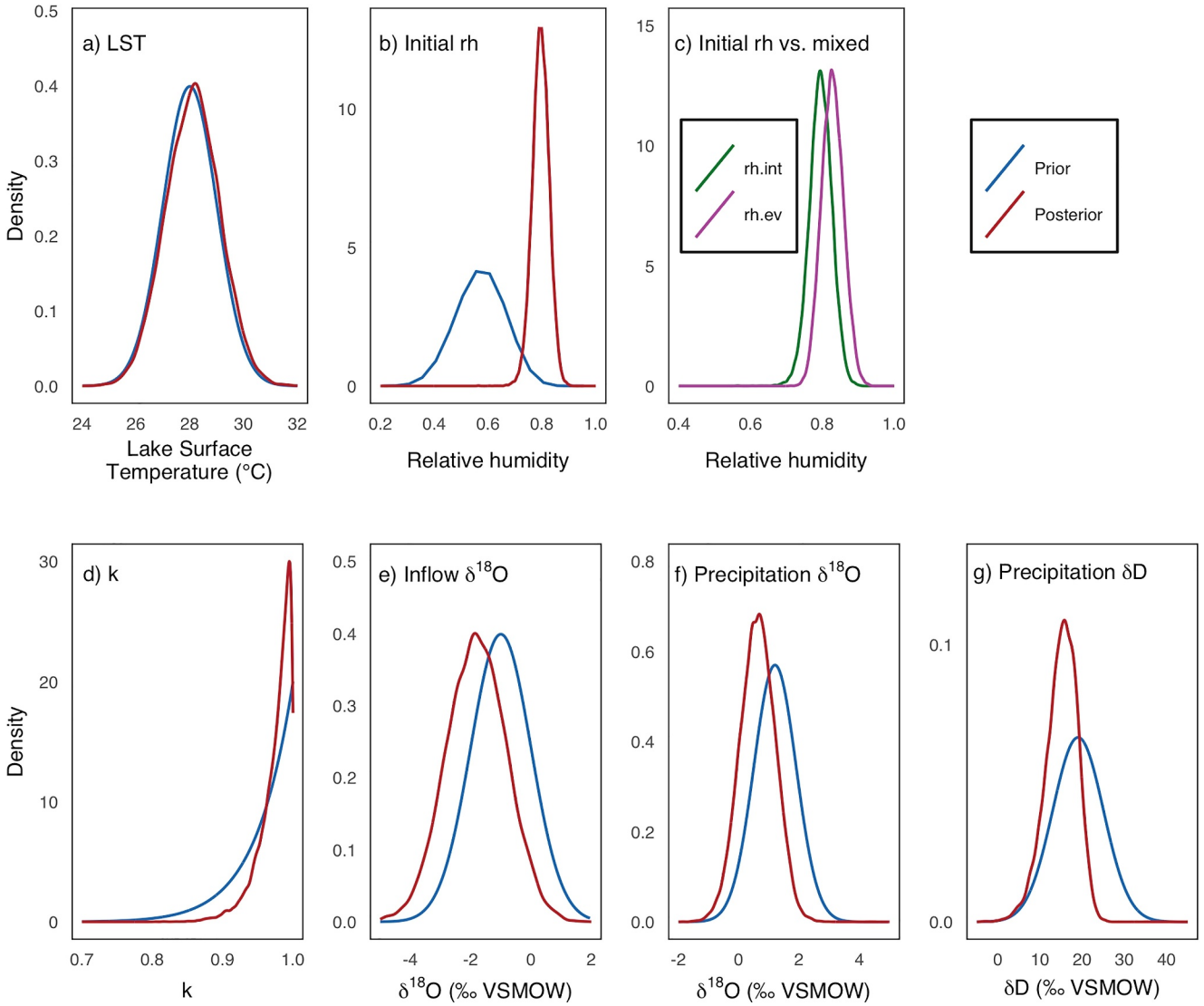

Figure 6. Comparisons between prior and posterior distributions in selected model parameters. LST (a) refers to lake surface temperature, *rh* is the relative humidity of the atmosphere overlying the lake water surface, *k* is a parameter describing the degree of isotope equilibrium between precipitation and water vapor isotope ratios (commonly assumed to be 1 in non-seasonal settings), and inflow $\delta^{18}O$ includes the mass balanced isotope value of all riverine inputs.

water isotope measurements at more latitudes, water vapor isotope measurements, and precipitation isotope measurements from over and immediately around the lake. Improving constraints on inflow water isotope values is especially important, and more measurements of the Omo River in particular would help refine the priors. Despite some uncertainties in model parameters and inconsistency between prior and posterior distributions, our results are encouraging in that the steady-state evaporation model is fairly consistent with our measured isotope values.

5.2. Model Applications and Future Studies

The LEL for Lake Turkana is a useful tool for interpreting lake water stable isotope ratios in the hot, arid, tropical environment of the basin. This data set represents the beginning of an ongoing campaign to regularly measure stable isotopes in and around the lake, and changes in the water balance may be detectable if measurements of lake water move along the LEL. Because of the difficulty of installing gauges and other instruments, the addition of this mass balance method is a valuable contribution to monitoring efforts. Including triple oxygen isotope analysis of archived and future samples would also inform our model assumptions, allowing for more in-depth

interpretations of moisture source and evaporative effects (Bershaw et al., 2020; Beverly et al., 2021; Passey & Ji, 2019).

Lake Turkana is not a source of drinking water for people, but it is linked to water resource questions through the rivers and dams in its basin. The data collection efforts initiated in the course of this study will produce time series isotope data for the Turkwel River, management of which is expected to adapt to a growing urban population, and for groundwater taps and wells. Droughts have occurred periodically for at least the last several million years, occasionally restricting availability of surface water including the Turkwel (Cohen et al., 2022). Present-day pastoralists dig both deep and shallow wells, access to which may be managed through longstanding cultural traditions (M'Mbogori et al., 2022). Shallow ground sources are more likely to be recharged during floods, but deep reservoirs that may sustain communities in times of drought contain ancient water that is not replenished on annual, decadal, or century timescales (Thomas et al., 2019). Unsustainable wastewater management practices and hydraulic fracturing also threaten the quality of groundwater accessible to local communities (Mbugua et al., 2022). Because deep and shallow groundwaters are isotopically distinct, regular isotope measurements of drinking water can provide insight into how groundwater consumption and management are affecting resource availability. Further, longitudinal monitoring efforts may be able to elucidate temporal or end-member mixing changes not captured by water chemistry or utilization rates alone.

The Bayesian approach to stable isotope mass balance of lakes should be tested in other systems. This method may provide the same utility in other lake systems and demonstrate similarities and differences between large lakes around the world. The focus on evaporation is especially relevant in arid zones, and the model can be expanded to evaluate mass balance in lakes with outflow (Gibson et al., 2016; Vystavna et al., 2021).

5.3. Consequences for Geologic Records and Paleohydrology

A comprehensive modern isotope hydrology data set and lake water isotope mass balance model will enable more detailed interpretations of paleohydrology from geological proxy data sets, including stable isotope measurements from lacustrine carbonates, soil carbonates, and fossil teeth.

Ostracods, microscopic crustaceans that live at the bottom of the lake and form calcium carbonate shells, provide some of the paleohydrology records for Lake Turkana (Beck et al., 2020; Feibel & Brown, 1992). Isotopic analysis of modern ostracods show a latitudinal trend of increasing ^{18}O enrichment with distance from the Omo River delta (Thirumalai et al., 2023), which was not observable in this study because of the infrequent and localized distribution of water sample collections. It would be difficult to establish a similar trend from our data set because the majority of our lake water samples represent the northern end of the lake (Figure 1). Consistent circulation, deposition, and upwelling patterns distribute water from its sources throughout the lake (Zăinescu et al., 2023), so we expect spatial variability in $\delta^{18}O$ to also remain consistent from year to year.

In the ecosystems surrounding the lake, small nodules of soil carbonate integrate climate signals over thousands to hundreds of thousands of years (Machette, 1985; Passey et al., 2010). Soil carbonates incorporate oxygen from meteoric water via soil water, and the mineralized oxygen is enriched in ^{18}O by evaporation in the soil column, then by fractionation during carbonate precipitation (Cerling & Quade, 1993). Paleosol water $\delta^{18}O$ can be calculated using carbonate $\delta^{18}O$ and estimates of formation temperature from clumped isotopes (Passey et al., 2010; Quade et al., 2013). In the Plio-Pleistocene Shungura and Nachukui Formations, mean estimated soil water is $\delta^{18}O = 1.07 \pm 0.6‰$ (1σ sd; Passey et al., 2010), slightly higher than present mean precipitation (Table 1). Modern soil water is prohibitively difficult to sample in Turkana given the infrequency of rain events sufficient to saturate the soil column, however soil water $\delta^{18}O$ can be calculated as a function of precipitation and surface water isotopes, depth, and rates of evaporation (Fischer-Femal & Bowen, 2021). Effects of evaporation vary from surface waters to soil water, but estimates of both are useful in evaluating aridity of a landscape (Beverly et al., 2021; Cerling & Quade, 1993). By comparing modern precipitation and surface waters with paleosol carbonates, which show a trend of aridification over the past 2 Ma (Levin et al., 2011; Passey et al., 2010), we can develop a water source history in Turkana and refine regional climate reconstructions. Developments in triple oxygen isotope analysis and modeling will further enhance the carbonate paleoclimate proxy, and availability of modern models and data for validation will be critical for improving proxy calibration (Jones et al., 2005; Kelson et al., 2017).

Much of the groundbreaking work in paleoecology in Turkana has focused on records from fossil teeth, establishing methods for estimating meteoric $\delta^{18}O$ through time by making comparisons between $\delta^{18}O$ in teeth of different animals (e.g., hippopotamids that live in the water vs. bovids that are not obligate drinkers) (Cerling et al., 2003). Together, the tooth enamel isotopes of multiple taxa provide an aridity index that enables a robust climate reconstruction (Levin et al., 2006). Increasingly sensitive analytical methods have enhanced the resolution of tooth enamel $\delta^{18}O$ to fine temporal scales that show seasonal changes in primate diets, indicating variability of water isotope composition across the landscape and over time (Green et al., 2022). Extending these records to modern times shows the shifts in regional climate conditions through the Neogene, and analyzing the effects of evaporation is particularly important for interpreting isotope measurements from the teeth of animals who may consume these evaporated waters.

New water isotope records for Lake Turkana and its watershed provide comparisons for paleo proxies that surround the fossils of our earliest ancestors. Variability of the lake and its fauna are part of the story of hominin evolution (Trauth et al., 2010), and in recent history, the timing of flood recession and harvest has been consistent enough for farmers and herders to structure their annual production cycles accordingly (Derbyshire et al., 2021). Now, geopolitics of resource management coupled with social and ecological change have altered these patterns. The lake has been vital to hominin communities for millions of years, and today more people than ever depend on it. As basin hydrology responds to rapid changes, analyzing stable isotopes from meteoric waters by modeling evaporative processes will provide a necessary dimension for understanding the effects of climate change on Lake Turkana. This record and the model approach establish a modern baseline for understanding this unique, water-limited environment.

Data Availability Statement

Previously published water isotope data are available as Supporting Information S1 with Levin et al. (2009). Lake Turkana height data courtesy of the USDA/NASA G-REALM program at (https://ipad.fas.usda.gov/cropexplorer/global_reservoir/). Precipitation records from TBI field stations is available via the Stony Brook University Academic Commons (Leakey et al., 2023). Version 0.1.3 of our "Bayesian approach for modeling Lake Turkana water isotopes" code is available on GitHub under a GNU General Public License v3.0, see Yang et al. (2024).

Acknowledgments

The authors thank Isaiah Nengo, Acacia Leakey, Martin Kirinya, Timothy Ngundo, Onesmus Kyalo Ngela, and Joseph Mutuku for facilitating the collection of waters at TBI. We also thank Hilary Sale, William Woto, Francis Ekai, Phillip Ekadeli, and Harrison Ngumbau for collecting many of the river, precipitation, and lake water samples. Samples from 2016 to 2018 were processed by Elizabeth Thomas and Owen Cowling in the Department of Geology at University at Buffalo, Buffalo NY. M.S. and G.H. were supported by NSF EAR 20-21579 with materials for this project provided by funding from Stony Brook University Department of Geosciences' David E. King Field Award, Stony Brook University startup funds to G.H., and the Turkana Basin Institute research fund (facilities support and funding). D.Y. was supported by the IDPAS doctoral research fund from Stony Brook University, and the Turkana Basin Institute Graduate Fellowship. D.L. and C.P. were supported by NSF EAR 20-20488.

References

Aron, P. G., Poulsen, C. J., Fiorella, R. P., Levin, N. E., Acosta, R. P., Yanites, B. J., & Cassel, E. J. (2021). Variability and controls on $\delta^{18}O$, d-excess, and $\Delta'^{17}O$ in southern Peruvian precipitation. *Journal of Geophysical Research: Atmospheres*, *126*(23), e2020JD034009. https://doi.org/10.1029/2020JD034009

Avery, S. (2010). *Hydrological impacts of Ethiopia's Omo Basin on Kenya's Lake Turkana water levels & fisheries*. African Development Bank.

Avery, S. (2012). *Lake Turkana & the lower Omo: Hydrological impacts of gibe III & lower Omo irrigation development*. University of Oxford African Studies Centre. Retrieved from https://www.africanstudies.ox.ac.uk/research-projects/lake-turkana-and-the-lower-omo-hydrological-impacts-of-major-dam-and-irrigation-de

Avery, S. (2014). What future for Lake Turkana and its wildlife? *Swara Magazine*, 24–30.

Beck, C. C., Feibel, C. S., Mortlock, R. A., Quinn, R. L., & Wright, J. D. (2020). Little ice age to modern lake-level fluctuations from Ferguson's Gulf, Lake Turkana, Kenya, based on sedimentology and ostracod assemblages. *Quaternary Research*, *101*, 1–14. https://doi.org/10.1017/qua.2020.105

Bedaso, Z. K., DeLuca, N. M., Levin, N. E., Zaitchik, B. F., Waugh, D. W., Wu, S.-Y., et al. (2020). Spatial and temporal variation in the isotopic composition of Ethiopian precipitation. *Journal of Hydrology*, *585*, 124364. https://doi.org/10.1016/j.jhydrol.2019.124364

Bershaw, J., Hansen, D. D., & Schauer, A. J. (2020). Deuterium excess and ^{17}O-excess variability in meteoric water across the Pacific Northwest, USA. *Tellus B: Chemical and Physical Meteorology*, *72*(1), 1–17. https://doi.org/10.1080/16000889.2020.1773722

Beverly, E. J., Levin, N. E., Passey, B. H., Aron, P. G., Yarian, D. A., Page, M., & Pelletier, E. M. (2021). Triple oxygen and clumped isotopes in modern soil carbonate along an aridity gradient in the Serengeti, Tanzania. *Earth and Planetary Science Letters*, *567*, 116952. https://doi.org/10.1016/j.epsl.2021.116952

Bloszies, C., Forman, S. L., & Wright, D. K. (2015). Water level history for Lake Turkana, Kenya in the past 15,000 years and a variable transition from the African humid period to Holocene aridity. *Global and Planetary Change*, *132*, 64–76. https://doi.org/10.1016/j.gloplacha.2015.06.006

Brooks, J. R., Wigington, P. J., Phillips, D. L., Comeleo, R., & Coulombe, R. (2012). Willamette River basin surface water isoscape ($\delta^{18}O$ and $\delta^{2}H$): Temporal changes of source water within the river. *Ecosphere*, *3*(5). https://doi.org/10.1890/ES11-00338.1

Carr, C. J. (2017). Components of catastrophe: Social and environmental consequences of Omo River basin development. In C. J. Carr (Ed.), *River basin development and human rights in Eastern Africa—A policy crossroads* (pp. 75–84). Springer International Publishing. https://doi.org/10.1007/978-3-319-50469-8_5

Cerling, T. E., Bowman, J. R., & O'Neil, J. R. (1988). An isotopic study of a fluvial-lacustrine sequence: The Plio-Pleistocene Koobi fora sequence, East Africa. *Palaeogeography, Palaeoclimatology, Palaeoecology*, *63*(4), 335–356. https://doi.org/10.1016/0031-0182(88)90104-6

Cerling, T. E., Harris, J. M., & Leakey, M. G. (2003). Isotope paleoecology of the Nowata and Nachukui formations at Lothagam, Turkana Basin, Kenya. In M. G. Leakey & J. M. Harris (Eds.), *Lothagam: The dawn of humanity in eastern Africa* (pp. 605–624). Columbia University Press. https://doi.org/10.7312/leak11870

Cerling, T. E., Levin, N. E., & Passey, B. H. (2011). Stable isotope ecology in the Omo-Turkana basin. *Evolutionary Anthropology: Issues, News, and Reviews*, *20*(6), 228–237. https://doi.org/10.1002/evan.20326

Cerling, T. E., & Quade, J. (1993). Stable carbon and oxygen isotopes in soil carbonates. In *Climate change in continental isotopic records* (pp. 217–231). AGU Books Board.

Cerling, T. E., Wynn, J. G., Andanje, S. A., Bird, M. I., Korir, D. K., Levin, N. E., et al. (2011). Woody cover and hominin environments in the past 6 million years. *Nature*, *476*(7358), 51–56. https://doi.org/10.1038/nature10306

Clark, I. D., & Fritz, P. (1997). *Environmental isotopes in hydrogeology* (1st ed.). CRC Press. Retrieved from https://mysite.science.uottawa.ca/eih/

Cohen, A. S., Du, A., Rowan, J., Yost, C. L., Billingsley, A. L., Campisano, C. J., et al. (2022). Plio-Pleistocene environmental variability in Africa and its implications for mammalian evolution. *Proceedings of the National Academy of Sciences of the United States of America*, *119*(16), e2107393119. https://doi.org/10.1073/pnas.2107393119

Craig, H. (1961). Atmospheric variations in meteoric waters. *Science*, *133*(3465), 1702–1703. https://doi.org/10.1126/science.133.3465.1702

Criss, R. E. (1999). *Principles of stable isotope distribution*. Oxford University Press.

Dansgaard, W. (1964). Stable isotopes in precipitation. *Tellus*, *16*(4), 436–468. https://doi.org/10.1111/j.2153-3490.1964.tb00181.x

Derbyshire, S. F., Nami, J. E., Akall, G., & Lowasa, L. (2021). Divining the future: Making sense of ecological uncertainty in Turkana, Northern Kenya. *Land*, *10*(9), 885. https://doi.org/10.3390/land10090885

Feibel, C. S. (2011). A geological history of the Turkana basin. *Evolutionary Anthropology: Issues, News, and Reviews*, *20*(6), 206–216. https://doi.org/10.1002/evan.20331

Feibel, C. S., & Brown, F. H. (1992). Microstratigraphy and paleoenvironments. In A. Walker & R. Leakey (Eds.), *The Nariokotome Homo erectus Skeleton* (pp. 21–39).

Fischer-Femal, B. J., & Bowen, G. J. (2021). Coupled carbon and oxygen isotope model for pedogenic carbonates. *Geochimica et Cosmochimica Acta*, *294*, 126–144. https://doi.org/10.1016/j.gca.2020.10.022

Forman, S. L., Wright, D. K., & Bloszies, C. (2014). Variations in water level for Lake Turkana in the past 8500 years near Mt. Porr, Kenya and the transition from the African Humid Period to Holocene aridity. *Quaternary Science Reviews*, *97*, 84–101. https://doi.org/10.1016/j.quascirev.2014.05.005

Garcin, Y., Melnick, D., Strecker, M. R., Olago, D., & Tiercelin, J.-J. (2012). East African mid-Holocene wet–dry transition recorded in palaeo-shorelines of Lake Turkana, northern Kenya Rift. *Earth and Planetary Science Letters*, *331–332*, 322–334. https://doi.org/10.1016/j.epsl.2012.03.016

Gat, J. R. (1995). Stable isotopes of fresh and saline lakes. In A. Lerman, D. M. Imboden, & J. R. Gat (Eds.), *Physics and chemistry of lakes* (2nd ed., pp. 139–165). Springer-Verlag.

Gat, J. R. (1996). Oxygen and hydrogen isotopes in the hydrologic cycle (Vol. *38*).

Gathogo, P. N., & Brown, F. H. (2006). Stratigraphy of the Koobi fora formation (Pliocene and Pleistocene) in the Ileret region of northern Kenya. *Journal of African Earth Sciences*, *45*(4–5), 369–390. https://doi.org/10.1016/j.jafrearsci.2006.03.006

Gibson, J. J., Birks, S. J., & Edwards, T. W. D. (2008). Global prediction of δA and δ^2H-δ^{18}O evaporation slopes for lakes and soil water accounting for seasonality. *Global Biogeochemical Cycles*, *22*(2). https://doi.org/10.1029/2007GB002997

Gibson, J. J., Birks, S. J., & Yi, Y. (2016). Stable isotope mass balance of lakes: A contemporary perspective. *Quaternary Science Reviews*, *131*, 316–328. https://doi.org/10.1016/j.quascirev.2015.04.013

Gownaris, N. J., Pikitch, E. K., Aller, J. Y., Kaufman, L. S., Kolding, J., Lwiza, K. M. M., et al. (2017). Fisheries and water level fluctuations in the world's largest desert lake. *Ecohydrology*, *10*(1), e1769. https://doi.org/10.1002/eco.1769

Gownaris, N. J., Rountos, K. J., Kaufman, L., Kolding, J., Lwiza, K. M. M., & Pikitch, E. K. (2018). Water level fluctuations and the ecosystem functioning of lakes. *Journal of Great Lakes Research*, *44*(6), 1154–1163. https://doi.org/10.1016/j.jglr.2018.08.005

Green, D. R., Ávila, J. N., Cote, S., Dirks, W., Lee, D., Poulsen, C. J., et al. (2022). Fine-scaled climate variation in equatorial Africa revealed by modern and fossil primate teeth. *Proceedings of the National Academy of Sciences of the United States of America*, *119*(35), e2123366119. https://doi.org/10.1073/pnas.2123366119

Harris, J. M., Cerling, T. E., Leakey, M. G., & Passey, B. H. (2008). Stable isotope ecology of fossil hippopotamids from the lake Turkana basin of east Africa. *Journal of Zoology*, *275*(3), 323–331. https://doi.org/10.1111/j.1469-7998.2008.00444.x

Hildebrand, E. A., Grillo, K. M., Sawchuk, E. A., Pfeiffer, S. K., Conyers, L. B., Goldstein, S. T., et al. (2018). A monumental cemetery built by eastern Africa's first herders near Lake Turkana, Kenya. *Proceedings of the National Academy of Sciences of the United States of America*, *115*(36), 8942–8947. https://doi.org/10.1073/pnas.1721975115

Hopson, A. J. (1982). *Lake Turkana: A report on the findings of the Lake Turkana project, 1972-1975* (p. 382). Government of Kenya and The Ministry of Overseas Development.

Horita, J., Rozanski, K., & Cohen, S. (2008). Isotope effects in the evaporation of water: A status report of the Craig–Gordon model. *Isotopes in Environmental and Health Studies*, *44*(1), 23–49. https://doi.org/10.1080/10256010801887174

Horita, J., & Wesolowski, D. J. (1994). Liquid-vapor fractionation of oxygen and hydrogen isotopes of water from the freezing to the critical temperature. *Geochimica et Cosmochimica Acta*, *58*(16), 3425–3437. https://doi.org/10.1016/0016-7037(94)90096-5

Horne, F. (2012). *What will happen if hunger comes?* Human Rights Watch. Retrieved from https://www.hrw.org/report/2012/06/18/what-will-happen-if-hunger-comes/abuses-against-indigenous-peoples-ethiopias

Jasechko, S. (2019). Global isotope hydrogeology——Review. *Reviews of Geophysics*, *57*(3), 835–965. https://doi.org/10.1029/2018RG000627

Johnson, T. C., & Malala, J. O. (2009). Lake Turkana and its link to the Nile. In *The Nile: Origin, environments, limnology, and human use*. Springer.

Jones, M. D., Leng, M. J., Roberts, C. N., Türkeş, M., & Moyeed, R. (2005). A coupled calibration and modelling approach to the understanding of dry-land Lake oxygen isotope records. *Journal of Paleolimnology*, *34*(3), 391–411. https://doi.org/10.1007/s10933-005-6743-0

Junqueira, A. B., Fernández-Llamazares, Á., Torrents-Ticó, M., Haira, P. L., Nasak, J. G., Burgas, D., et al. (2021). Interactions between climate change and infrastructure projects in changing water resources: An ethnobiological Perspective from the Daasanach, Kenya. *Journal of Ethnobiology*, *41*(3), 331–348. https://doi.org/10.2993/0278-0771-41.3.331

Kelson, J. R., Huntington, K. W., Schauer, A. J., Saenger, C., & Lechler, A. R. (2017). Toward a universal carbonate clumped isotope calibration: Diverse synthesis and preparatory methods suggest a single temperature relationship. *Geochimica et Cosmochimica Acta*, *197*, 104–131. https://doi.org/10.1016/j.gca.2016.10.010

Kolding, J. (1992). A summary of Lake Turkana: An ever-changing mixed environment. In *SIL Communications, 1953-1996* (Vol. 23, pp. 25–35). https://doi.org/10.1080/05384680.1992.11904005

Lahr, M. M., Rivera, F., Power, R. K., Mounier, A., Copsey, B., Crivellaro, F., et al. (2016). Inter-group violence among early Holocene hunter-gatherers of West Turkana, Kenya. *Nature*, *529*(7586), 394–398. https://doi.org/10.1038/nature16477

Leakey, A., Henkes, G., Saslaw, M., & Martins, D. (2023). Precipitation recorded in the Turkana Basin from 2005 to 2022 [Dataset]. *Geosciences Research Data*. Retrieved from https://commons.library.stonybrook.edu/geodata/8

Levin, N. E., Brown, F. H., Behrensmeyer, A. K., Bobe, R., & Cerling, T. E. (2011). Paleosol carbonates from the Omo Group: Isotopic records of local and regional environmental change in East Africa. *Palaeogeography, Palaeoclimatology, Palaeoecology*, *307*(1–4), 75–89. https://doi.org/10.1016/j.palaeo.2011.04.026

Levin, N. E., Cerling, T. E., Passey, B. H., Harris, J. M., & Ehleringer, J. R. (2006). A stable isotope aridity index for terrestrial environments. *Proceedings of the National Academy of Sciences of the United States of America*, *103*(30), 11201–11205. https://doi.org/10.1073/pnas.0604719103

Levin, N. E., Zipser, E. J., & Cerling, T. E. (2009). Isotopic composition of waters from Ethiopia and Kenya: Insights into moisture sources for eastern Africa [Dataset]. *Journal of Geophysical Research*, *114*(D23). https://doi.org/10.1029/2009JD012166

Lunn, D., Jackson, C., Best, N., Thomas, A., & Spiegelhalter, D. (2012). *The BUGS book: A practical introduction to Bayesian analysis*. Chapman & Hall. Retrieved from https://www.routledge.com/The-BUGS-Book-A-Practical-Introduction-to-Bayesian-Analysis/Lunn-Jackson-Best-Thomas-Spiegelhalter/p/book/9781584888499

Lupien, R. L., Russell, J. M., Grove, M., Beck, C. C., Feibel, C. S., & Cohen, A. S. (2020). Abrupt climate change and its influences on hominin evolution during the early Pleistocene in the Turkana Basin, Kenya. *Quaternary Science Reviews*, *245*, 106531. https://doi.org/10.1016/j.quascirev.2020.106531

Machette, M. N. (1985). *Calcic soils of the southwestern United States (No. 203)*. Geological Society of America.

Mbugua, D., Makokha, M. K., & Shisanya, C. A. (2022). Assessment of physicochemical properties of groundwater near oil well pads in Lokichar Basin, Turkana County, Kenya. *Open Access Library Journal*, *9*(3), 1–17. https://doi.org/10.4236/oalib.1108487

M'Mbogori, F. N., Kinyua, M. G., Ibrae, A. G., & Lane, P. J. (2022). Changes to water management and declining pastoral resilience in Marsabit County, northern Kenya: The example of Gabra wells. *WIREs Water*, *9*(6). https://doi.org/10.1002/wat2.1609

Morley, C. K., Karanja, F. M., Wescott, W. A., Stone, D. M., Harper, R. M., Wigger, S. T., & Day, R. A. (1999). Geology and geophysics of the western Turkana basins, Kenya. In C. K. Morley (Ed.), *Geoscience of rift systems—Evolution of East Africa*. American Association of Petroleum Geologists. https://doi.org/10.1306/St44623C2

Morrissey, A., Scholz, C. A., & Russell, J. M. (2017). Late Quaternary TEX86 paleotemperatures from the world's largest desert lake, Lake Turkana, Kenya. *Journal of Paleolimnology*, *59*(1), 103–117. https://doi.org/10.1007/s10933-016-9939-6

Munday, C., Engelstaedter, S., Ouma, G., Ogutu, G., Olago, D., Ong'ech, D., et al. (2022). Observations of the Turkana jet and the East African dry tropics: The RIFTJet field campaign. *Bulletin of the American Meteorological Society*, *103*(8), E1828–E1842. https://doi.org/10.1175/BAMS-D-21-0214.1

Nicholson, S. E. (1996). A review of climate dynamics and climate variability in eastern Africa. In T. C. Johnson, E. O. Odada, & K. T. Whittaker (Eds.), *The limnology, climatology and paleoclimatology of the East African Lakes*. Taylor & Francis Group. https://doi.org/10.1201/9780203748978

Nicholson, S. E. (2016). The Turkana low-level jet: Mean climatology and association with regional aridity. *International Journal of Climatology*, *36*(6), 2598–2614. https://doi.org/10.1002/joc.4515

Nicholson, S. E. (2022). Lake-effect rainfall over Africa's great lakes and other lakes in the rift valleys. *Journal of Great Lakes Research*, *49*(6), 101971. https://doi.org/10.1016/j.jglr.2021.12.004

Obiero, K., Wakjira, M., Gownaris, N. J., Malala, J., Keyombe, J. L., Ajode, M. Z., et al. (2022). Lake Turkana: Status, challenges, and opportunities for collaborative research. *Journal of Great Lakes Research*, *49*(6), 102120. https://doi.org/10.1016/j.jglr.2022.10.007

Olaka, L. A., Odada, E. O., Trauth, M. H., & Olago, D. O. (2010). The sensitivity of East African rift lakes to climate fluctuations. *Journal of Paleolimnology*, *44*(2), 629–644. https://doi.org/10.1007/s10933-010-9442-4

Passey, B. H., & Ji, H. (2019). Triple oxygen isotope signatures of evaporation in lake waters and carbonates: A case study from the western United States. *Earth and Planetary Science Letters*, *518*, 1–12. https://doi.org/10.1016/j.epsl.2019.04.026

Passey, B. H., Levin, N. E., Cerling, T. E., Brown, F. H., & Eiler, J. M. (2010). High-temperature environments of human evolution in East Africa based on bond ordering in paleosol carbonates. *Proceedings of the National Academy of Sciences*, *107*(25), 11245–11249. https://doi.org/10.1073/pnas.1001824107

Quade, J., Eiler, J., Daëron, M., & Achyuthan, H. (2013). The clumped isotope geothermometer in soil and paleosol carbonate. *Geochimica et Cosmochimica Acta*, *105*, 92–107. https://doi.org/10.1016/j.gca.2012.11.031

Rasbury, E. T., Present, T. M., Northrup, P., Tappero, R. V., Lanzirotti, A., Cole, J. M., et al. (2021). Tools for uranium characterization in carbonate samples: Case studies of natural U–Pb geochronology reference materials. *Geochronology*, *3*(1), 103–122. https://doi.org/10.5194/gchron-3-103-2021

Ricketts, R. D., & Johnson, T. C. (1996). Climate change in the Turkana basin as deduced from a 4000 year long δO^{18} record. *Earth and Planetary Science Letters*, *142*(1), 7–17. https://doi.org/10.1016/0012-821X(96)00094-5

Rozanski, K., Araguás-Araguás, L., & Gonfiantini, R. (1992). Isotopic patterns in modern global precipitation. *Journal of Geophysical Research*, *78*, 1–36. https://doi.org/10.1029/GM078p0001

Schapper, A. (2021). Climate Justice concerns and human rights trade-offs in Ethiopia's Green economy transition: The case of Gibe III. *European Journal of Development Research*, *33*(6), 1952–1972. https://doi.org/10.1057/s41287-020-00340-6

Tanui, F., Olago, D., Ouma, G., & Kuria, Z. (2023). Hydrochemical and isotopic characteristics of the Lodwar Alluvial Aquifer System (LAAS) in Northwestern Kenya and implications for sustainable groundwater use in dryland urban areas. *Journal of African Earth Sciences*, *206*, 105043. https://doi.org/10.1016/j.jafrearsci.2023.105043

Thirumalai, K., Cohen, A. S., & Taylor, D. (2023). Hydrologic controls on individual ostracode stable isotopes in a desert lake: A modern baseline for Lake Turkana. *Geochemistry, Geophysics, Geosystems*, *24*(5), e2022GC010790. https://doi.org/10.1029/2022GC010790

Thomas, E. A., Needoba, J., Kaberia, D., Butterworth, J., Adams, E. C., Oduor, P., et al. (2019). Quantifying increased groundwater demand from prolonged drought in the East African Rift Valley. *Science of the Total Environment*, *666*, 1265–1272. https://doi.org/10.1016/j.scitotenv.2019.02.206

Tierney, J. E., Lewis, S. C., Cook, B. I., LeGrande, A. N., & Schmidt, G. A. (2011). Model, proxy and isotopic perspectives on the East African Humid Period. *Earth and Planetary Science Letters*, *307*(1–2), 103–112. https://doi.org/10.1016/j.epsl.2011.04.038

Trauth, M. H., Maslin, M. A., Deino, A. L., Junginger, A., Lesoloyia, M., Odada, E. O., et al. (2010). Human evolution in a variable environment: The amplifier lakes of eastern Africa. *Quaternary Science Reviews*, *29*(23–24), 2981–2988. https://doi.org/10.1016/j.quascirev.2010.07.007

UNESCO. (2018). Lake Turkana National Parks (Kenya) inscribed on list of world heritage in danger [Dataset]. *UNESCO*. Retrieved from https://whc.unesco.org/en/news/1842/

USDA/NASA G-REALM. (2023). Lake Turkana (000093) height variations from TOPEX/POSEIDON and Jason series altimetry [Dataset]. *USDA/NASA G-REALM*. Retrieved from https://ipad.fas.usda.gov/cropexplorer/global_reservoir/gr_regional_chart_jason1.aspx?regionid=eafrica&reservoir_name=Turkana&lakeid=000093

van der Lubbe, H. J. L., Krause-Nehring, J., Junginger, A., Garcin, Y., Joordens, J. C. A., Davies, G. R., et al. (2017). Gradual or abrupt? Changes in water source of Lake Turkana (Kenya) during the African Humid Period inferred from Sr isotope ratios. *Quaternary Science Reviews*, *174*, 1–12. https://doi.org/10.1016/j.quascirev.2017.08.010

van Geldern, R., & Barth, J. A. C. (2012). Optimization of instrument setup and post-run corrections for oxygen and hydrogen stable isotope measurements of water by isotope ratio infrared spectroscopy (IRIS). *Limnology and Oceanography: Methods*, *10*(12), 1024–1036. https://doi.org/10.4319/lom.2012.10.1024

Vizy, E. K., & Cook, K. H. (2019). Observed relationship between the Turkana low-level jet and boreal summer convection. *Climate Dynamics*, *53*(7–8), 4037–4058. https://doi.org/10.1007/s00382-019-04769-2

Vystavna, Y., Harjung, A., Monteiro, L. R., Matiatos, I., & Wassenaar, L. I. (2021). Stable isotopes in global lakes integrate catchment and climatic controls on evaporation. *Nature Communications*, *12*(1), 7224. https://doi.org/10.1038/s41467-021-27569-x

Wood, B., & Leakey, M. (2011). The Omo-Turkana basin fossil hominins and their contribution to our understanding of human evolution in Africa. *Evolutionary Anthropology: Issues, News, and Reviews*, *20*(6), 264–292. https://doi.org/10.1002/evan.20335

Wynn, J. G. (2000). Paleosols, stable carbon isotopes, and paleoenvironmental interpretation of Kanapoi, Northern Kenya. *Journal of Human Evolution*, *39*(4), 411–432. https://doi.org/10.1006/jhev.2000.0431

Yang, D., Saslaw, M., & Henkes, G. (2024). Bayesian approach for modeling Lake Turkana water isotopes [Software]. *Zenodo*. https://doi.org/10.5281/zenodo.10668927

Yost, C. L., Lupien, R. L., Beck, C., Feibel, C. S., Archer, S. R., & Cohen, A. S. (2021). Orbital influence on precipitation, fire, and grass community composition from 1.87 to 1.38 Ma in the Turkana Basin, Kenya. *Frontiers in Earth Science*, *9*. https://doi.org/10.3389/feart.2021.568646

Yuretich, R. F., & Cerling, T. E. (1983). Hydrogeochemistry of Lake Turkana, Kenya: Mass balance and mineral reactions in an alkaline lake. *Geochimica et Cosmochimica Acta*, *47*(6), 1099–1109. https://doi.org/10.1016/0016-7037(83)90240-5

Zăinescu, F., van der Vegt, H., Storms, J., Nutz, A., Bozetti, G., May, J.-H., et al. (2023). The role of wind-wave related processes in redistributing river-derived terrigenous sediments in Lake Turkana: A modelling study. *Journal of Great Lakes Research*, *49*(2), 368–386. https://doi.org/10.1016/j.jglr.2022.12.013

References From the Supporting Information

Bowen, G. J. (2024). The online isotopes in precipitation calculator (version 3.1) [Software]. *Waterisotopes.org*. Retrieved from http://www.waterisotopes.org

Bowen, G. J., & Revenaugh, J. (2003). Interpolating the isotopic composition of modern meteoric precipitation. *Water Resources Research*, *39*(10). https://doi.org/10.1029/2003WR002086

Craig, H., & Gordon, L. I. (1965). Deuterium and oxygen 18 variations m the ocean and the marine atmosphere (Vol. *63*).

Curtis, S. M., Goldin, I., & Evangelou, E., & GitHub, "sumtxt" from. (2018). mcmcplots: Create plots from MCMC output (version 0.4.3) [Software]. *CRAN-R*. Retrieved from https://cran.r-project.org/web/packages/mcmcplots/index.html

Daux, V., Minster, B., Cauquoin, A., Jossoud, O., Werner, M., & Landais, A. (2021). Oxygen and hydrogen isotopic composition of tap waters in France. *Geological Society, London, Special Publications*, *507*(1), 47–61. https://doi.org/10.1144/SP507-2020-207

Gabry, J., & Mahr, T. (2024). bayesplot: Plotting for Bayesian models (version 1.11.0). Retrieved from https://mc-stan.org/bayesplot/

Gabry, J., Simpson, D., Vehtari, A., Betancourt, M., & Gelman, A. (2019). Visualization in Bayesian workflow. *Journal of the Royal Statistical Society - Series A: Statistics in Society*, *182*(2), 389–402. https://doi.org/10.1111/rssa.12378

Gelman, A., & Rubin, D. B. (1992). Inference from iterative simulation using multiple sequences. *Statistical Science*, *7*(4), 457–472. https://doi.org/10.1214/ss/1177011136

IAEA/WMO. (2020). Global network of isotopes in precipitation. Retrieved from https://nucleus.iaea.org/wiser/index.aspx

Jasechko, S., Gibson, J. J., & Edwards, T. W. D. (2014). Stable isotope mass balance of the Laurentian great lakes. *Journal of Great Lakes Research*, *40*(2), 336–346. https://doi.org/10.1016/j.jglr.2014.02.020

Källqvist, T., Lien, L., & Liti, D. (1988). *Lake Turkana limnological study 1985-1988 (No. D-R5313)*. Norwegian Institute for Water Research & Kenya Marine and Fisheries Research Institute.

Konecky, B., Dee, S. G., & Noone, D. C. (2019). WaxPSM: A forward model of leaf wax hydrogen isotope ratios to bridge proxy and model estimates of past climate. *Journal of Geophysical Research: Biogeosciences*, *124*(7), 2107–2125. https://doi.org/10.1029/2018JG004708

Makowski, D., Ben-Shachar, M. S., & Lüdecke, D. (2019). bayestestR: Describing effects and their uncertainty, existence and significance within the Bayesian Framework. *Journal of Open Source Software*, *4*(40), 1541. https://doi.org/10.21105/joss.01541

National Oceanic and Atmospheric Administration. (1990). Lodwar climate normals 1961–1990 [Dataset]. *National Oceanic and Atmospheric Administration*. Retrieved from https://www.ncei.noaa.gov/products/wmo-climate-normals

Plummer, M. (2023). JAGS: Just another Gibbs sampler [Software]. *MCMC*. Retrieved from https://sourceforge.net/projects/mcmc-jags/

R Core Team. (2023). R: A language and environment for statistical computing (version 4.3.2) [Software]. *R Foundation for Statistical Computing*. Retrieved from https://www.R-project.org/

Spigel, R. H., & Coulter, G. W. (1996). Comparison of hydrology and physical limnology of the East African great lakes: Tanganyika, Malawi, Victoria, Kivu and Turkana (with reference to some north American great lakes). In T. C. Johnson, E. O. Odada, & K. T. Whittaker (Eds.), *The limnology, climatology and paleoclimatology of the East African Lakes*. Taylor & Francis Group. https://doi.org/10.1201/9780203748978

Su, Y.-S., & Yajima, M. (2024). R2jags: Using R to run "JAGS" (version 0.7-1.1) [Software]. *CRAN-R*. Retrieved from https://cran.r-project.org/web/packages/R2jags/index.html

Wang, S., Zhang, M., Bowen, G. J., Liu, X., Du, M., Chen, F., et al. (2018). Water source signatures in the spatial and seasonal isotope variation of Chinese tap waters. *Water Resources Research*, *54*(11), 9131–9143. https://doi.org/10.1029/2018WR023091